Self Assembled, Sulfonated Pentablock Copolymer Cation Exchange Coatings for Membrane Capacitive Deionization

Journal:	*Molecular Systems Design & Engineering*
Manuscript ID	ME-ART-12-2018-000115.R1
Article Type:	Paper
Date Submitted by the Author:	31-Jan-2019
Complete List of Authors:	Jain, Amit; Rice University, Chemical and Biomolecular Engineering Weathers, Cierra; Rice University, Chemical and Biomolecular Engineering Kim, Jun; Rice University, Civil and Environmental Engineering Meyer, Matthew; Rice University, Shared Equipment Authority Walker, Shane; University of Texas at El Paso, Civil Engineering Li, Qilin; Rice University, Civil and Environmental Eng Verduzco, Rafael; Rice University, Chemical and Biomolecular Engineering

Self Assembled, Sulfonated Pentablock Copolymer Cation Exchange Coatings for Membrane Capacitive Deionization

Amit Jain[1,2], Cierra Weathers[1,2], Jun Kim[2,3], Matthew D. Meyer[5], Shane Walker[2,6], Qilin Li[2,3], Rafael Verduzco[1,2,4,]*

[1]Department of Chemical and Biomolecular Engineering, Rice University, MS 362, 6100 Main Street, Houston, USA

[2]NSF Nanosystems Engineering Research Center Nanotechnology-Enabled Water Treatment, Rice University, MS 6398, 6100 Main Street, Houston, USA

[3]Civil and Environmental Engineering, Rice University, MS 319, 6100 Main Street, Houston, USA

[4]Material Science and Nanoengineering, Rice University, MS 325, 6100 Main Street, Houston, USA

[5]Shared Equipment Authority, Rice University, MS 100, 6100 Main Street, Houston, USA

[6]Civil Engineering, The University of Texas at El Paso, 500 W University Avenue, El Paso, Texas, USA

Correspondence to: rafaelv@rice.edu,

Keywords: Capacitive Deionization, Membrane, Sulfonated pentablock copolymer, Activated Carbon, Desalination.

Abstract

Membrane capacitive deionization (MCDI) is a simple and low-cost method for brackish water desalination involving reversible electrosorption using high surface area, porous electrodes paired with ion-exchange membranes. Ion-exchange membranes improve charge efficiency and salt adsorption capacity by limiting the transport of co-ions and inhibiting faradaic reactions at the electrode surface. Effective ion-exchange membranes for MCDI should have high permselectivity and low ionic resistance, but there is typically a trade-off between these two properties. In this work, we studied partially sulfonated pentablock copolymer (sPBC) as a cation-exchange coating for MCDI electrodes. sPBC ion exchange coatings of varying ion exchange capacity (IEC, 1.0, 1.5, 2.0 meq/g) and a range of casting solvent compositions (10 – 60 wt % *n*-propanol in toluene) were prepared. Transmission electron microscopy analysis of the membranes showed a morphological change from a micellar to lamellar and then to an inverse micellar structure with increasing polarity of the casting solvent. Water uptake and salt permeability increased with increasing IEC and casting solvent polarity over the entire range of conditions tested. MCDI device studies indicated that charge efficiency and salt adsorption capacity both increased with water uptake over a range of casting solvent compositions due to morphological changes in the sPBC film. This work demonstrates an effective solution-processible ion-exchange layer for MCDI using a self-assembling block copolymer and suggests that ideal ion-exchange coatings for MCDI should have high water uptake to minimize ionic resistance while at the same time maintaining a high charge density of fixed charged groups to achieve a high permselectivity.

Introduction

Water scarcity is a challenge in regions across the globe,[1,2] and simple, low-cost methods for desalination of brackish ground waters can help address the need for clean water[3]. Various desalination technologies have been deployed successfully for groundwater desalination including multi-stage flash distillation, multi-effect distillation, reverse osmosis (RO), and electrodialysis [2,4–6]. RO represents the largest segment (64%) of the global desalination capacity followed by thermal (31%) and electrochemical methods (4%)[4], but limitations of RO include a high energy consumption (1.5 – 2.5 kW h/m^3) for low salinity feed waters[1,4], susceptibility to scaling and fouling, and low water recoveries.[6–8]

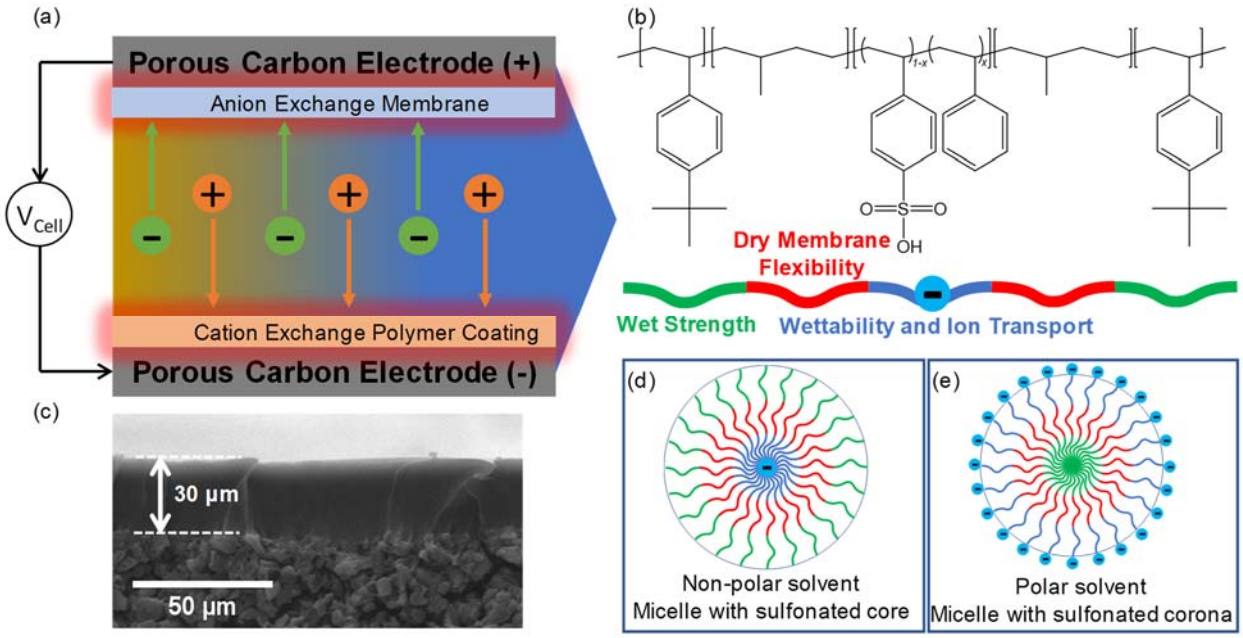

Figure 1. (a) Schematic of electrosorption in an MCDI device, (b) chemical structure and schematic of the sulfonated pentablock copolymer (sPBC), (c) cross-sectional SEM photograph of an sPBC-coated electrode, and schematics for anticipated solution morphologies of sPBC in (d) non-polar solvent, and (e) polar solvent.

Electrochemical methods provide an alternative, simple and scalable route to desalination. Membrane capacitive deionization (MCDI) is an electrosorption technique involving porous electrodes along with ion exchange membranes or coatings, as shown in **Figure 1a**. Ions are removed from the feed stream on application of a voltage and subsequently discharged when the voltage is removed or inverted, enabling recovery of some of the energy during the uptake step. The use of ion exchange membranes (IEMs) improves salt adsorption capacity and energy efficiency by preventing passage of co-ions between the feed solution and electrode surfaces[9–15] and inhibiting faradaic reactions on the surface of the electrodes[16–18].

The performance of an MCDI module depends strongly on the properties of ion-exchange membranes, in particular the permselectivity and salt permeability. The permselectivity describes the preferential transport of cations over anions, or vice-versa, and the permeability describes the rate of transport across the membrane. Both of these properties are often in conflict, and prior studies have shown that increasing permeability (or reducing resistance) will reduce permselectivity, and vice-versa[19]. Here, we explore a solution-processible, sulfonated pentablock copolymer (sPBC) as a cation-exchange polymer for MCDI. The material can be cast as a thin, uniform layer, providing an attractive method to control ion transport while minimizing interfacial resistance[20,21]. As we demonstrate below, the use of a self-assembling block copolymer system enables tuning of permeability, permselectivity, and morphology with casting conditions. Prior work with block copolymer ion exchange membranes for MCDI is limited and has typically focused on hydrophobic materials with low water uptake and sulfonation levels[11,22–25]. The materials studied here have water uptake capacities exceeding 200 % relative to the dry polymer films.

Sulfonated pentablock copolymers with the product name Nexar™ (see **Figure 1b**) have been studied for various applications including water treatment[26], desalination[27,28] and pervaporation[29,30]. These materials are attractive as ion-exchange coatings for CDI due to their

tunable hydrophilicity, good ion transport properties, and exceptional mechanical properties. Further, the ability to easily process these materials as thin films over porous electrodes is attractive for the scalable production of CDI modules. Fundamental studies performed by Choi et al.[31] showed that when dissolved in non-polar solvent the polymer chains aggregate to form micelles with polar segment (SPS, sulfonated polystyrene) in the micelle core and non-polar segment (tBS-HI, tertiary butyl styrene-hydrogenated isoprene) in corona as depicted schematically in **Figure 1d**. They also demonstrated that the as-cast solid-state films retained the micellar morphologies and have continuous sulfonated domains at higher sulfonation levels[32]. Griffin et al.[33] studied the solution morphology of these polymers by varying the solvent polarity and observed spherical micelles with sulfonated core (**Figure 1d**) at low polarity, dissolved polymer chains at neutral polarity, and inverse micelles with sulfonated corona at high solvent polarity (**Figure 1e**). Zheng and Cornelius[34] and Truong et al.[35] studied the effect of the solvent blend polarity on the film morphology, and their results suggested that upon casting from a relatively polar solvent these polymer films consist of well-connected sulfonated domains which leads to significant increase in the water uptake and proton conductivity.

Here, we present a study of sPBCs as cation-exchange membranes for MCDI. sPBCs of varying ion exchange capacity and casting solvent polarity were analyzed with respect to water uptake, salt permeability, morphology, and performance as ion-exchange coatings for MCDI. Large changes in water uptake and salt permeability coincided with morphological transitions observed by transmission electron microscopy (TEM). An optimal casting solvent composition was identified which maximized salt adsorption capacity and charge efficiency. In contrast to other ion-exchange membranes studied, water uptake and salt permeability both increased with water uptake over a range of casting solvent compositions due to morphological changes in the sPBC film. This study

demonstrates a viable block copolymer material for use as a thin film ion-exchange coating for membrane capacitive deionization.

Materials and Methods

Materials

Activated carbon CEP21K (surface area 2040 m^2/g) was purchased from Power Carbon Technology Co., Ltd. Graphite sheets of 0.005-inch thickness (Mineral Seal Corporation, USA) were used as current collectors. AMX/CMX membranes (electrical resistance 2.0/3.0 Ω cm^2 and thickness 140/170 μm) were purchased from ASTOM-Neosepta. Polyvinyl alcohol (PVA, fully hydrolyzed, M_w = 89,000 – 98,000 g/mol), glutaraldehyde (GA, 25 wt % solution in water), and toluene and *n*-propanol solvents were purchased from Sigma Aldrich and used as received. Deionized water (E-Pure, resistivity 18 Mohm) was used for the synthesis of the electrodes and preparation of polymer and salt solutions. The sulfonated pentablock copolymers (sPBC) used in this work were generously provided by the Kraton Polymers, LLC, Houston. The sPBC polymer is a pentablock copolymer comprised of *tert*-butyl styrene (tBS) end-blocks, partially sulfonated polystyrene (SPS) mid-block, hydrogenated isoprene (HI) spacer blocks between the SPS and tBS blocks. The molecular weight of the unsulfonated polymer is 15 kg/mol for the tBS endblocks, 10 and 20 kg/mol for each HI spacer block, and 28 kg/mol for the SPS mideblock. Three different samples with 26, 39, and 52 mol % sulfonation levels corresponding to the ion-exchange capacities of 1.0 meq/g, 1.5 meq/g and 2.0 meq/g were studied. Detailed descriptions of the polymer synthesis and structure can be found elsewhere[31,36].

Activated Carbon electrode

Aqueous processed activated carbon electrodes were prepared as reported previously[37]. Briefly, activated carbon powder (90 wt %, dry basis) was mixed with the poly(vinyl alcohol) (PVA,

10 wt % dry basis) aqueous solution along with the glutaraldehyde aqueous solution (GA, 5 mol% with respect to PVA repeat units). Here PVA acts as the electrode binder and GA as the crosslinker for the hydrophilic PVA chains. The prepared mixture was mixed overnight to obtain a homogeneous slurry, flow-coated onto a graphite current collector, and dried. The electrode was subsequently coated with the sPBC as descried below.

Preparation and Deposition of sPBC IEM

For casting, sPBCs (15 wt %) were dissolved in a mixture of toluene and *n*-propanol. The solution was cast over activated carbon electrodes by flow-coating using a gap-height of 200 μm. Once coated with the polymer solution, the electrodes were dried overnight to ensure the complete removal of the solvent followed by thermal annealing in the oven at 130 ^{o}C for one hour to complete the crosslinking of the electrode binder. Free-standing polymer films were prepared by casting the polymer solution onto mylar sheets.

MCDI Desalination tests

Desalination tests were carried out using a flow-by type CDI cell using a configuration described previously[38]. A 10 mM NaCl feed solution was used for all experiments described, and the voltage was cycled between 1.2 V and 0 V during desalination and regeneration steps, respectively. The cycle times were 1000 s for both adsorption and desorption, and the water flow rate was kept constant at 1 mL/minute, corresponding to a retention time of 36 seconds.

*Salt Adsorption Capacity (*SAC*):* The SAC represents the mass of salt removed from the feed stream during one adsorption cycle normalized by the total mass of the electrode, including carbon and binder:

$$\text{SAC} = \frac{Q * \int_{t_0}^{t_{ads}} (C_o - C_t) dt}{W_{electrode}} \qquad (1)$$

where Q is the volumetric flow rate (1 mL/min, fixed), t_0 and t_{ads} are the cycle initiation time and adsorption cycle completion time, C_o and C_t are the feed and instantaneous effluent concentration respectively in mg/L and $W_{electrode}$ is the electrode mass.

Charge Efficiency: The charge efficiency of the system is ratio of the moles of the salt removed per mole of the electrical charge supplied during the adsorption cycle.

$$\text{Charge Efficiency} = \frac{\left(Q * \int_{t_0}^{t_{ads}} (C_o - C_t) dt / m\right)}{\left(\int_{t_0}^{t_{ads}} I * dt / F\right)} \qquad (2)$$

Where, m is the molecular weight of the salt (58.44 g/mol NaCl) and F is Faraday's constant (96485 C/eq).

Water uptake: Water uptake represents the mass fraction of water in a swollen film and was measured by the gravimetric method[27]. A free-standing polymer film prepared as described above was submerged in DI water and allowed to sit overnight. Next, the polymer film was removed from the water, the surface was dried by gently blotting with tissue, and the mass of the hydrated film was measured. The measurement was repeated three times for each sample.

Salt permeability: Salt permeability tests were conducted to determine the effect of water uptake on the mobile ion transport[27] using a diffusion cell set up[27]. The setup consists of two glass chambers containing either test solution (donor cell, 10 mM NaCl) or DI water (receiver cell), as shown in the Supporting Information **Figure S1**. The two chambers are separated by a hydrated sPBC film. The conductivity of the receiver cell was monitored continuously using a conductivity probe, and the

measured conductivity was converted into salt concentration using the standard calibration value (10mM NaCl, 1100 μS/cm).

The salt permeability was calculated using the following equation[27].

$$\ln\left[1 - 2\frac{C_R[t]}{C_D[0]}\right] = -2\,\frac{A}{VL}\boldsymbol{P_s}t \qquad (5)$$

Where, $C_D[0]$ and $C_R[t]$ are the donor cell initial salt concentration (10 mM) and the receiver cell salt concentration at time t, A is the effective cross-sectional area of the membrane (1.77 cm^2), V is the chamber volume (25 mL each), L is the membrane thickness measured after the test, and P_s is the calculated salt permeability. The P_s values reported correspond to steady state salt concentration, which was achieved after two hours of operation.

Film Morphology Analysis Using Transmission Electron Microscopy (TEM)

Freestanding film samples were sectioned at a thickness of 100 nm at room temperature using an ultramicrotome (Leica EM UC7, Leica Microsystems, Germany). Sections were stained with OsO_4 vapor emitted from 1% OsO_4 solution for 12 hours in a sealed chamber, then rinsed in deionized water. The vapors will stain the tBS-HI part of the chain, and hence it will appear electron dense in the image. After completely drying at room temperature, samples were analyzed using TEM (JEM-1230, JEOL, Japan) operating with an accelerating voltage of 80 kV. Some films were observed to have artifacts after staining due to crystallization of OsO_4 on the electrode surface. The block copolymer domains can be clearly resolved in these images, and they are presented in the Supporting Information. After extensively washing these films with DI water, most of the artifacts from staining were removed. Images after additional washing are presented in the main manuscript.

Scanning Electron Microscopy (SEM)

Ion-exchange polymer coated electrodes were analyzed by scanning electron microscopy (SEM, FEI Quanta 400) using a cross-sectional mode. Samples were sputtered with a thin layer of gold prior to analysis. For cross-sectional analysis, electrodes were fractured after freezing in liquid nitrogen and mounted on an SEM mount.

Results

Prior to testing in MCDI devices, free-standing sPBC films of varying ion-exchange capacities (IECs) of 1.0, 1.5, and 2.0 were cast from a 15 wt % polymer solution prepared in 1:1 mixture of toluene and *n*-propanol. As-prepared films were characterized with respect to water uptake and salt permeability, and the results are shown in **Figure 2a**. As expected[28,39], both water uptake and salt permeability increased significantly with increasing ion exchange capacity. Relative to the dry sPBC membranes, water uptake varied from 36 % for IEC of 1.0 up to 200 wt % for IEC 2.0. The salt permeability increased by more than a factor of 4 with increasing IEC from 1.0 to 2.0. This is expected due to the increased hydrophilicity with increasing IEC and is consistent with prior reports[28]. These water uptake values (up to 200%) and salt permeability ($4x10^{-7}$ cm^2/s) values are significantly higher than the typical values (up to 100% and $1x10^{-7}$ cm^2/s) reported in the literature for other ion-exchange materials used for MCDI[27,28,40,39].

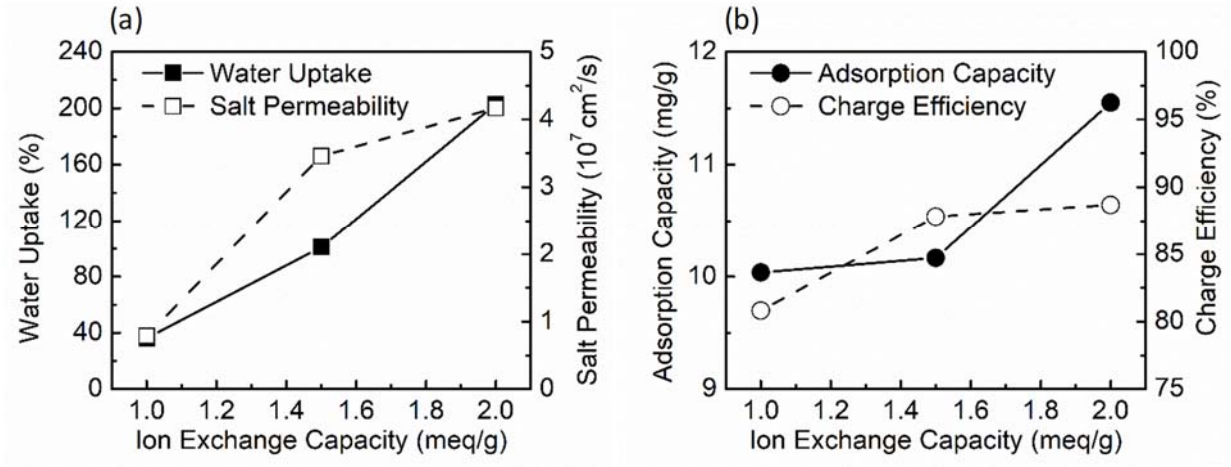

Figure 2. (a) Water uptake and salt permeability (P_s), and (b) salt adsorption capacity (SAC) and charge efficiency as a function of ion-exchange capacity.

Next, the sPBCs of varying ion-exchange capacities (1.0, 1.5, and 2.0) were tested as cation exchange coatings for MCDI. In all MCDI devices tested, anodes were comprised of a porous carbon electrode along with a commercial anion exchange membrane. Cathodes were comprised of porous carbon electrodes coated with an sPBC polymer layer of approximately 30 μm thickness (see **Figure 1c**). The performance of sPBC-coated electrodes was compared to that of cathodes paired with a commercial cation exchange membrane (CEM). Desalination tests were conducted using a 10 mM (584 mg/L) NaCl solution, a common salinity used for MCDI studies and applications[41]. Voltages for adsorption and regeneration were 1.2 and 0 V, respectively, and tests were conducted for at least 30 continuous cycles. Representative uptake and regeneration cycles are included in the Supporting Information **Figure S2** along with the salt adsorption capacities and charge efficiencies for all devices tested (Supporting Information **Figures S3 – S4**).

Both salt adsorption capacity (SAC) and charge efficiency increase with IEC, as shown in **Figure 2b**. Interestingly, the SAC increases only slightly with IEC from 1.0 to 1.5 and more strongly with IEC from 1.5 to 2.0. Conversely, the charge efficiency increases strongly with IEC from 1.0 to 1.5 and only slightly with IEC from 1.5 to 2.0. The small increase in charge efficiency at higher IEC may reflect a trade-off between water uptake and permselectivity. Increased water uptake reduces the local concentration of sulfonic acid groups, impacting the resulting charge efficiency. This suggests that increasing the water uptake further could be detrimental to charge efficiency due to further dilution of the sulfonic acid groups.

Prior work[33–35,42] has shown that simply varying the polarity of the casting solvent can impact the physical properties of sPBCs. As shown schematically in **Figures 1d and e**, we expected

that increasing polarity could cause the sPBC morphology to transition from micelles with a hydrophilic core and hydrophobic corona to inverted micelles with hydrophilic coronas, resulting in a more hydrophilic film after casting.

To investigate the change in morphology with casting solvent polarity, TEM analysis of the cation exchange membranes was performed as a function of casting solvent polarity. We focused on the sPBC with IEC of 2.0, which exhibited the best performance in MCDI devices, and the casting solution used in this work was a mixture of toluene (non-polar solvent) and *n*-propanol (polar solvent). The casting solvent composition was varied from 10 to 60 wt % *n*-propanol. The resulting films were sectioned, stained, and analyzed by TEM. As shown in **Figure 3**, an initially micellar morphology at 10 % *n*-propanol transitions to lamellar (20 and 30 %) and then an inverted micellar phase (40 – 60 %). These observations are consistent with prior reports on these materials in which the effect of casting solvent was studied[33–35,42]. Additional TEM images with improved contrast between the block copolymer domains (along with some artifacts due to crystallization of OsO_4) are presented in the Supporting Information **Figure S6**, and the morphology observed in these additional images is consistent with the morphology presented in **Figure 3**. We additionally conducted TEM analysis of the sPBC polymer films of varying IECs (Supporting Information **Figure S5**), and these studies revealed and inverted micellar morphology for all the three IECs when cast from 50 % *n*-propanol solvent mixture.

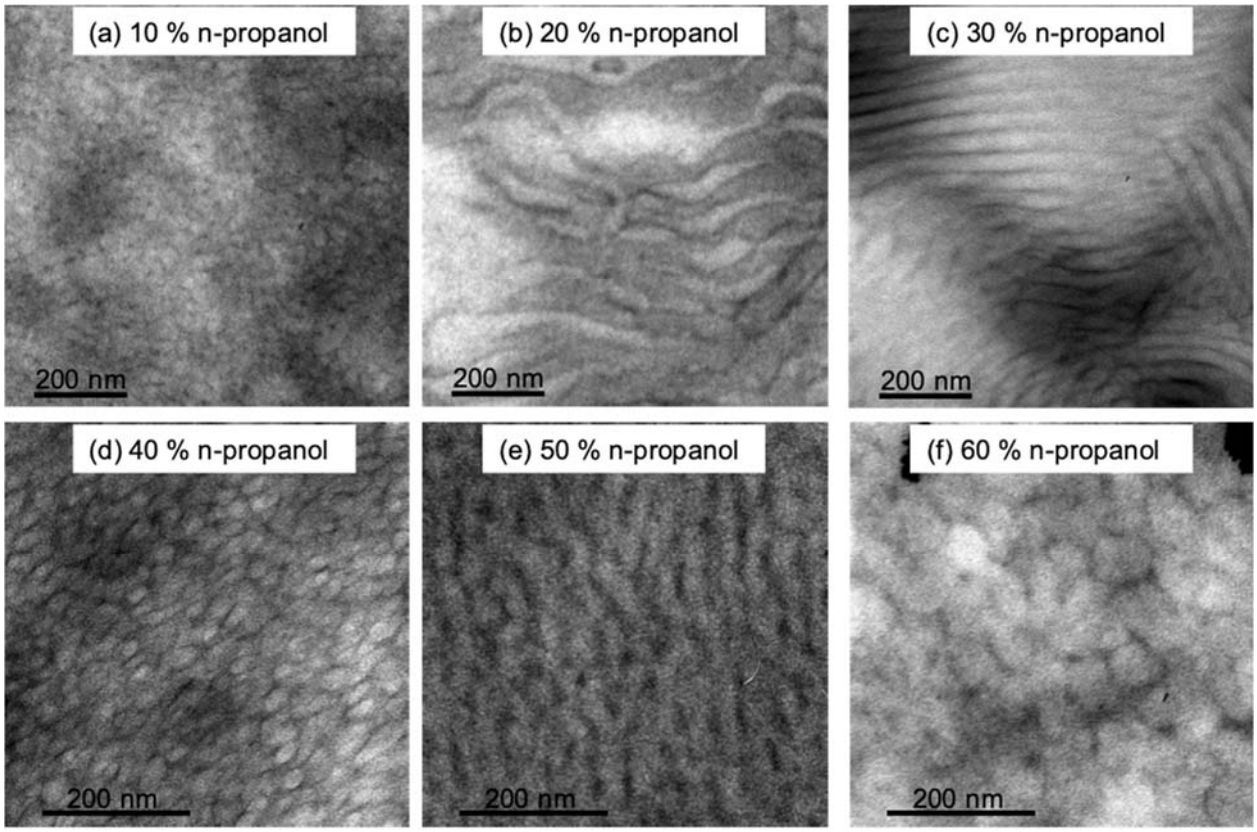

Figure 3. TEM images demonstrating the morphology of the polymer films when cast form the casting solvent blend with (a) 10 wt % *n*-propanol, (b) 20 wt % *n*-propanol, (c) 30 wt % *n*-propanol, (d) 40 wt % *n*-propanol, (e) 50 wt % *n*-propanol, and (f) 60 wt % *n*-propanol. All the casting solutions were prepared from IEC 2.0.

The water uptake and salt permeability were measured as a function of the casting solvent composition for the sPBC with an IEC of 2.0 meq/g. As shown in **Figure 4a**, water uptake and salt permeability generally increased with increasing casting solution content of *n*-propanol. This can be attributed to the increasing size and connectivity of hydrophilic domains with increasing casting solvent polarity.[32] Increasing the polarity of the solvent resulted in morphological transitions of the sPBC film from a micellar (**Figure 3 a**) to a lamellar (**Figure 3 b and c**), and then an inverted micellar (**Figure 3 d-f**) phase, the latter with a continuous hydrophilic domain. It is unclear why the

water uptake and permeability are lower at 20 % *n*-propanol compared with 10 %, but this may be due to the morphological transition that occurs over this composition range of casting solvent.

Next, the performance of sPBCs was evaluated in MCDI devices. Based on prior reports of ion-exchange coatings and the relationship between water uptake and permselectivity, we would expect a decrease in charge efficiency with increasing water uptake due to a reduction in permselectivity[19]. Contrary to that, over the range of 10 to 40% *n*-propanol content, the SAC and charge efficiency increase with increasing casting solvent polarity. The charge efficiency decreases for *n*-propanol casting solvent content above 40 %, and the SAC increases from 40 to 50% and then also decreases with increasing solvent polarity.

The observed increase in charge efficiency and SAC with increasing solvent polarity up to 40 wt *% n*-propanol indicate an increasing salt permeability and permselectivity over this range of casting solvents. We attribute the increase in permselectivity to increased exposure of sulfonic acid groups in the sPBC layer when the sPBC is cast from a more polar solvent. The reduction in charge efficiency above 40 % *n*-propanol reflects a reduction in permselectivity, which we attribute to dilution of the sulfonic acid groups[19]. The reduced SAC (or cation uptake) above 50 wt % *n*-propanol is attributed to a reduced permselectivity, or effectiveness of the sPBC in blocking passage of anions through the sPBC layer.

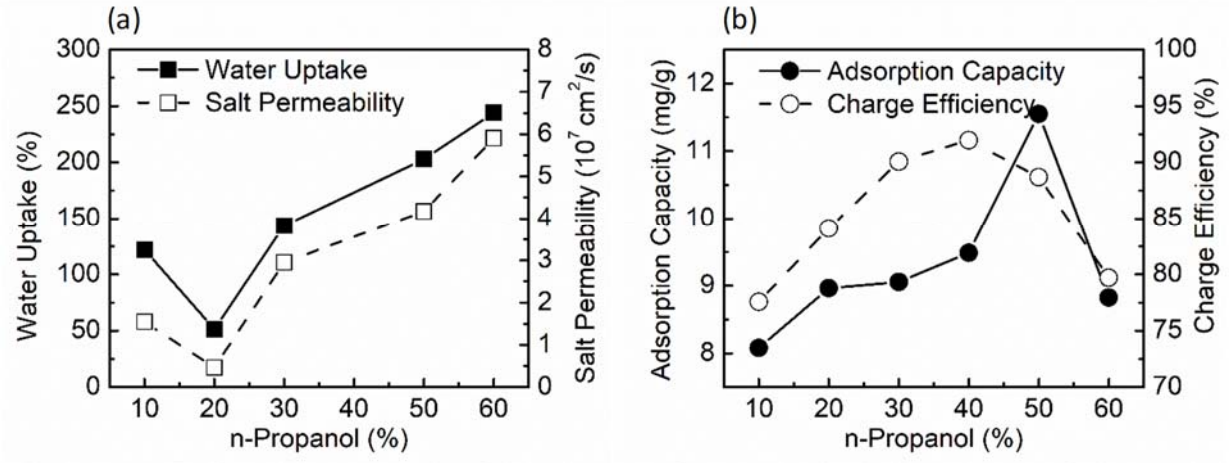

Figure 4. (a) Water uptake and salt permeability and (b) salt adsorption capacity and charge efficiency as a function of casting solvent composition.

Discussion

We conducted morphological and transport measurements of sPBC ion-exchange layers and studied the performance of MCDI devices using sPBC as a cation-exchange coating. TEM analysis revealed a transition from a micellar, to a lamellar, and finally an inverted micellar morphology with increasing solvent polarity, and a schematic for the changing sPBC morphology with casting solvent content is shown in **Figure 5**. The maximum salt adsorption capacity (11.5 mg/g) and charge efficiency (92%) obtained for MCDI with an sPBC-coated cathode were comparable to that of the MCDI device with commercial IEMs (12 mg/g, 87.6 %, see Supporting Information **Table S1**).

We observe clear trade-offs in the water-uptake, salt-adsorption capacity, and charge efficiency for MCDI devices with sPBC as cation exchange membranes. The water uptake for sPBC with 2.0 IEC was tunable through variation of the casting solvent polarity, from approximately 100 to 250 wt % water uptake. At both the highest and lowest water uptake values, salt adsorption capacities and charge efficiencies are poor, as reflected in **Figure 4**. Low water uptake impedes ion transport, while high water uptake dilutes the concentration of sulfonic acids groups and reduces permselectivity. Optimal performance was found at an intermediate value of water uptake, achieved through systematic variation of the casting solvent polarity.

This work demonstrates an effective solution-processible ion-exchange layer for MCDI using a self-assembling block copolymer with tunable morphology, water uptake, and performance by varying casting conditions. Our work suggests that ideal ion-exchange coatings for MCDI should

have high water uptake to minimize ionic resistance while at the same time maintaining a high charge density of fixed charged groups to achieve a high permselectivity.

.

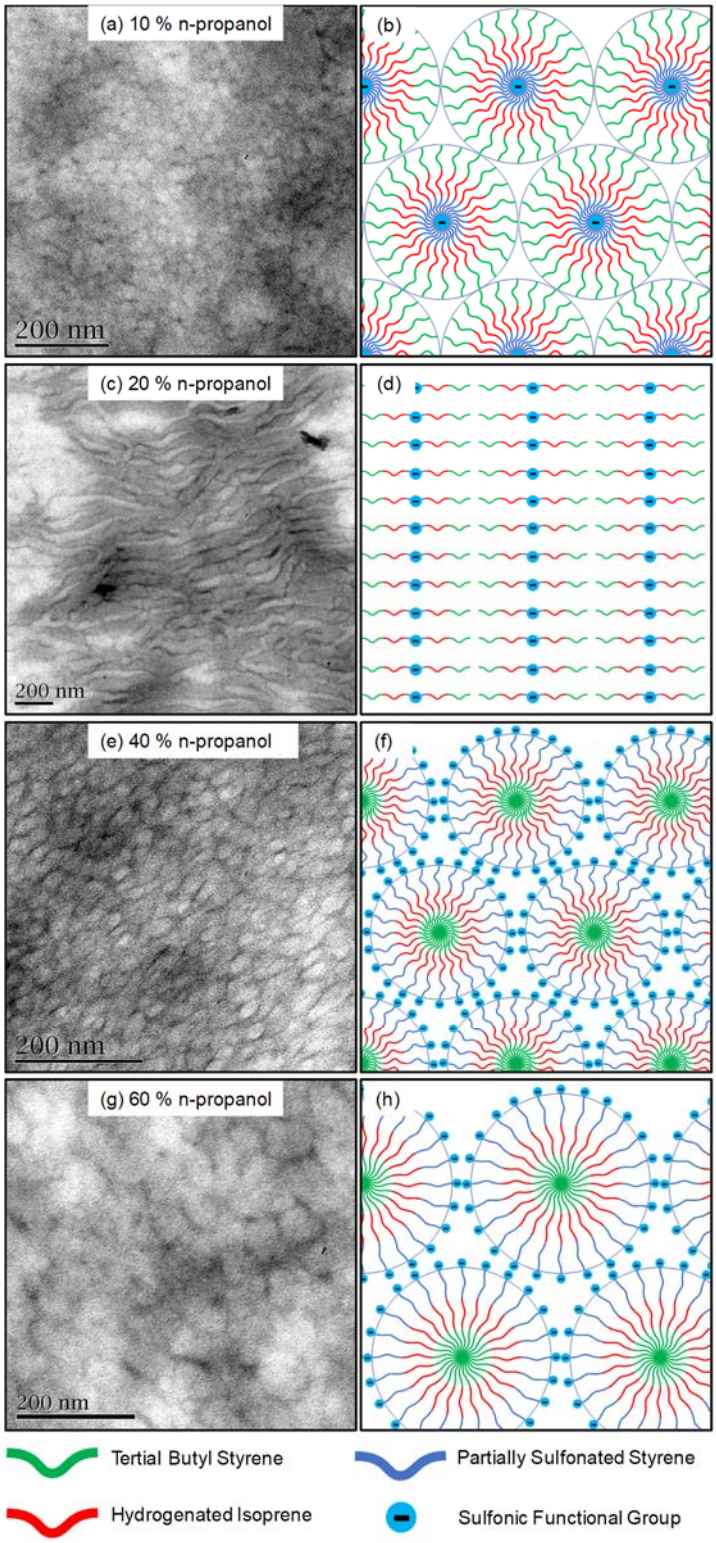

Figure 5. Schematics for morphological transition in sPBC layers along with corresponding TEM images of sPBC film prepared at different casting solvent compositions.

Associated Content

Supporting Information. Additional details on the salt permeability tests setup, plot for effluent concentration for 5 stable cycles, plots for 30 cycles data on salt adsorption capacity and charge efficiency, TEM images for various polymer films with different ion-exchange capacities and tabulated data on water uptake, salt permeability, salt adsorption capacity and charge efficiency are provided in the Supporting Information. This information is available free of charge via the Internet at http://pubs.acs.org.

Author Information

Corresponding Author: Rafael Verduzco, rafaelv@rice.edu

Present Address: 6100 Main Street, MS 362, Houston, TX 77005

Funding Sources

National Science Foundation (NEWT EEC-1449500, CBET-1604666) and the Welch Foundation for Chemical Research (C-1888).

ACKNOWLEDGEMENT

This work was supported by the National Science Foundation Nanosystems Engineering Research Center for Nanotechnology Enabled Water Treatment (NEWT EEC 1449500), NEWT Center Research Experience for Undergraduates EEC-1449500, National Science Foundation CBET-1604666, and the Welch Foundation for Chemical Research (C-1888).

ABBREVIATIONS

CDI, Capacitive Deionization; MCDI, Membrane Capacitive Deionization; IEC, ion-exchange capacity; SAC, Salt Adsorption Capacity; PVA, Polyvinyl Alcohol; GA, Glutaraldehyde;IEM, Ion-exchange Membrane; sPBCs, sulfonated pentablock copolymers; tBS, *tert*-butyl styrene; SPS, sulfonated polystyrene; HI, hydrogenated isoprene.

References

(1) Humplik, T.; Lee, J.; O'Hern, S. C.; Fellman, B. A.; Baig, M. A.; Hassan, S. F.; Atieh, M. A.; Rahman, F.; Laoui, T.; Karnik, R.; et al. Nanostructured Materials for Water Desalination. *Nanotechnology* **2011**, *22* (29), 292001. https://doi.org/10.1088/0957-4484/22/29/292001.

(2) Imbrogno, J.; Belfort, G. Membrane Desalination: Where Are We, and What Can We Learn from Fundamentals? *Annu. Rev. Chem. Biomol. Eng.* **2016**, *7*, 29–64. https://doi.org/10.1146/annurev-chembioeng-061114-123202.

(3) Stanton, J. S.; Dennehy, K. F. *Brackish Groundwater and Its Potential to Augment Freshwater Supplies*; Fact Sheet; USGS Numbered Series 2017-3054; U.S. Geological Survey: Reston, VA, 2017.

(4) AlMarzooqi, F. A.; Al, G.; Saadat, I.; Hilal, N. Application of Capacitive Deionisation in Water Desalination: A Review. *Desalination* **2014**, *342*, 3–15. https://doi.org/10.1016/j.desal.2014.02.031.

(5) Al-Karaghouli, A.; Kazmerski, L. L. Energy Consumption and Water Production Cost of Conventional and Renewable-Energy-Powered Desalination Processes. *Renew. Sustain. Energy Rev.* **2013**, *24*, 343–356. https://doi.org/10.1016/j.rser.2012.12.064.

(6) Shannon, M. A.; Bohn, P. W.; Elimelech, M.; Georgiadis, J. G.; Mariñas, B. J.; Mayes, A. M. Science and Technology for Water Purification in the Coming Decades. *Nature* **2008**, *452* (7185), 301–310. https://doi.org/10.1038/nature06599.

(7) Antony, A.; Low, J. H.; Gray, S.; Childress, A. E.; Le-Clech, P.; Leslie, G. Scale Formation and Control in High Pressure Membrane Water Treatment Systems: A Review. *J. Membr. Sci.* **2011**, *383* (1–2), 1–16. https://doi.org/10.1016/j.memsci.2011.08.054.

(8) Werber, J. R.; Osuji, C. O.; Elimelech, M. Materials for next-Generation Desalination and Water Purification Membranes. *Nat. Rev. Mater.* **2016**, *1* (5), 16018. https://doi.org/10.1038/natrevmats.2016.18.

(9) Kim, Y.-J.; Choi, J.-H. Enhanced Desalination Efficiency in Capacitive Deionization with an Ion-Selective Membrane. *Sep. Purif. Technol.* **2010**, *71* (1), 70–75. https://doi.org/10.1016/j.seppur.2009.10.026.

(10) Biesheuvel, P. M.; Zhao, R.; Porada, S.; van der Wal, A. Theory of Membrane Capacitive Deionization Including the Effect of the Electrode Pore Space. *J. Colloid Interface Sci.* **2011**, *360* (1), 239–248. https://doi.org/10.1016/j.jcis.2011.04.049.

(11) Ji Sun Kim; Kim, C. S.; Shin, H. S.; Rhim, J. W. Application of Synthesized Anion and Cation Exchange Polymers to Membrane Capacitive Deionization (MCDI). *Macromol. Res.* **2015**, *23* (4), 360–366. https://doi.org/10.1007/s13233-015-3049-6.

(12) Lee, J.-B.; Park, K.-K.; Eum, H.-M.; Lee, C.-W. Desalination of a Thermal Power Plant Wastewater by Membrane Capacitive Deionization. *Desalination* **2006**, *196* (1–3), 125–134. https://doi.org/10.1016/j.desal.2006.01.011.

(13) Li, H.; Zou, L. Ion-Exchange Membrane Capacitive Deionization: A New Strategy for Brackish Water Desalination. *Desalination* **2011**, *275* (1–3), 62–66. https://doi.org/10.1016/j.desal.2011.02.027.

(14) Kim, T.; Gorski, C. A.; Logan, B. E. Low Energy Desalination Using Battery Electrode Deionization. *Environ. Sci. Technol. Lett.* **2017**, *4* (10), 444–449. https://doi.org/10.1021/acs.estlett.7b00392.

(15) Zuo, K.; Kim, J.; Jain, A.; Wang, T.; Verduzco, R.; Long, M.; Li, Q. Novel Composite Electrodes for Selective Removal of Sulfate by the Capacitive Deionization Process. *Environ. Sci. Technol.* **2018**, *52* (16), 9486–9494. https://doi.org/10.1021/acs.est.8b01868.

(16) Hassanvand, A.; Wei, K.; Talebi, S.; Chen, G. Q.; Kentish, S. E. The Role of Ion Exchange Membranes in Membrane Capacitive Deionisation. *Membranes* **2017**, *7* (3), 54. https://doi.org/10.3390/membranes7030054.

(17) Zhang, C.; He, D.; Ma, J.; Tang, W.; Waite, T. D. Faradaic Reactions in Capacitive Deionization (CDI) - Problems and Possibilities: A Review. *Water Res.* **2018**, *128* (Supplement C), 314–330. https://doi.org/10.1016/j.watres.2017.10.024.

(18) Omosebi, A.; Gao, X.; Landon, J.; Liu, K. Asymmetric Electrode Configuration for Enhanced Membrane Capacitive Deionization. *ACS Appl. Mater. Interfaces* **2014**, *6* (15), 12640–12649. https://doi.org/10.1021/am5026209.

(19) Geise, G. M.; Hickner, M. A.; Logan, B. E. Ionic Resistance and Permselectivity Tradeoffs in Anion Exchange Membranes. *ACS Appl. Mater. Interfaces* **2013**, *5* (20), 10294–10301. https://doi.org/10.1021/am403207w.

(20) Kim, J.-S.; Choi, J.-H. Fabrication and Characterization of a Carbon Electrode Coated with Cation-Exchange Polymer for the Membrane Capacitive Deionization Applications. *J. Membr. Sci.* **2010**, *355* (1–2), 85–90. https://doi.org/10.1016/j.memsci.2010.03.010.

(21) Kim, Y.-J.; Choi, J.-H. Improvement of Desalination Efficiency in Capacitive Deionization Using a Carbon Electrode Coated with an Ion-Exchange Polymer. *Water Res.* **2010**, *44* (3), 990–996. https://doi.org/10.1016/j.watres.2009.10.017.

(22) Lee, J.-Y.; Seo, S.-J.; Yun, S.-H.; Moon, S.-H. Preparation of Ion Exchanger Layered Electrodes for Advanced Membrane Capacitive Deionization (MCDI). *Water Res.* **2011**, *45* (17), 5375–5380. https://doi.org/10.1016/j.watres.2011.06.028.

(23) Kim, J. S.; Jeon, Y. S.; Rhim, J. W. Application of Poly(vinyl Alcohol) and Polysulfone Based Ionic Exchange Polymers to Membrane Capacitive Deionization for the Removal of Mono- and Divalent Salts. *Sep. Purif. Technol.* **2016**, *157*, 45–52. https://doi.org/10.1016/j.seppur.2015.11.011.

(24) Kwak, N.-S.; Koo, J. S.; Hwang, T. S.; Choi, E. M. Synthesis and Electrical Properties of NaSS–MAA–MMA Cation Exchange Membranes for Membrane Capacitive Deionization (MCDI). *Desalination* **2012**, *285* (Supplement C), 138–146. https://doi.org/10.1016/j.desal.2011.09.046.

(25) Asquith, B. M.; Meier-Haack, J.; Ladewig, B. P. Cation Exchange Copolymer Enhanced Electrosorption. *Desalination* **2014**, *345*, 94–100. https://doi.org/10.1016/j.desal.2014.04.027.

(26) Filice, S.; D'Angelo, D.; Scarangella, A.; Iannazzo, D.; Compagnini, G.; Scalese, S. Highly Effective and Reusable Sulfonated Pentablock Copolymer Nanocomposites for Water Purification Applications. *RSC Adv.* **2017**, *7* (72), 45521–45534. https://doi.org/10.1039/C7RA08000J.

(27) Geise, G. M.; Freeman, B. D.; Paul, D. R. Sodium Chloride Diffusion in Sulfonated Polymers for Membrane Applications. *J. Membr. Sci.* **2013**, *427*, 186–196. https://doi.org/10.1016/j.memsci.2012.09.029.

(28) Geise, G. M.; Freeman, B. D.; Paul, D. R. Characterization of a Sulfonated Pentablock Copolymer for Desalination Applications. *Polymer* **2010**, *51* (24), 5815–5822. https://doi.org/10.1016/j.polymer.2010.09.072.

(29) Shi, G. M.; Zuo, J.; Tang, S. H.; Wei, S.; Chung, T. S. Layer-by-Layer (LbL) Polyelectrolyte Membrane with Nexar™ Polymer as a Polyanion for Pervaporation Dehydration of Ethanol. *Sep. Purif. Technol.* **2015**, *140*, 13–22. https://doi.org/10.1016/j.seppur.2014.11.008.

(30) Zuo, J.; Shi, G. M.; Wei, S.; Chung, T.-S. The Development of Novel Nexar Block Copolymer/Ultem Composite Membranes for C2–C4 Alcohols Dehydration via Pervaporation. *ACS Appl. Mater. Interfaces* **2014**, *6* (16), 13874–13883. https://doi.org/10.1021/am503277t.

(31) Choi, J.-H.; Kota, A.; Winey, K. I. Micellar Morphology in Sulfonated Pentablock Copolymer Solutions. *Ind. Eng. Chem. Res.* **2010**, *49* (23), 12093–12097. https://doi.org/10.1021/ie1002476.

(32) Choi, J.-H.; Willis, C. L.; Winey, K. I. Structure–property Relationship in Sulfonated Pentablock Copolymers. *J. Membr. Sci.* **2012**, *394–395*, 169–174. https://doi.org/10.1016/j.memsci.2011.12.036.

(33) Griffin, P. J.; Salmon, G. B.; Ford, J.; Winey, K. I. Predicting the Solution Morphology of a Sulfonated Pentablock Copolymer in Binary Solvent Mixtures. *J. Polym. Sci. Part B Polym. Phys.* **2016**, *54* (2), 254–262. https://doi.org/10.1002/polb.23914.

(34) Zheng, W.; Cornelius, C. J. Solvent Tunable Multi-Block Ionomer Morphology and Its Relationship to Modulus, Water Swelling, Directionally Dependent Ion Transport, and

Actuator Performance. *Polymer* **2016**, *103*, 104–111. https://doi.org/10.1016/j.polymer.2016.09.055.

(35) Truong, P. V.; Shingleton, S.; Kammoun, M.; Black, R. L.; Charendoff, M.; Willis, C.; Ardebili, H.; Stein, G. E. Structure and Properties of Sulfonated Pentablock Terpolymer Films as a Function of Wet–Dry Cycles. *Macromolecules* **2018**, *51* (6), 2203–2215. https://doi.org/10.1021/acs.macromol.8b00194.

(36) Willis, C. L.; Jr, D. L. H.; Trenor, S. R.; Mather, B. D. Sulfonated Block Copolymers, Method for Making Same, and Various Uses for Such Block Copolymers. US7737224 B2, June 15, 2010.

(37) Jain, A.; Kim, J.; Owoseni, O. M.; Weathers, C.; Caña, D.; Zuo, K.; Walker, W. S.; Li, Q.; Verduzco, R. Aqueous-Processed, High-Capacity Electrodes for Membrane Capacitive Deionization. *Environ. Sci. Technol.* **2018**, *52* (10), 5859–5867. https://doi.org/10.1021/acs.est.7b05874.

(38) Jain, A.; Kim, J.; Owoseni, O. M.; Weathers, C.; Cana, D.; Zuo, K.; Walker, W. S.; Li, Q.; Verduzco, R. Aqueous-Processed, High-Capacity Electrodes for Membrane Capacitive Deionization. *Environ. Sci. Technol.* **2018**. https://doi.org/10.1021/acs.est.7b05874.

(39) Geise, G. M.; Paul, D. R.; Freeman, B. D. Fundamental Water and Salt Transport Properties of Polymeric Materials. *Prog. Polym. Sci.* **2014**, *39* (1), 1–42. https://doi.org/10.1016/j.progpolymsci.2013.07.001.

(40) Geise, G. M.; Falcon, L. P.; Freeman, B. D.; Paul, D. R. Sodium Chloride Sorption in Sulfonated Polymers for Membrane Applications. *J. Membr. Sci.* **2012**, *423–424*, 195–208. https://doi.org/10.1016/j.memsci.2012.08.014.

(41) Porada, S.; Zhao, R.; van der Wal, A.; Presser, V.; Biesheuvel, P. M. Review on the Science and Technology of Water Desalination by Capacitive Deionization. *Prog. Mater. Sci.* **2013**, *58* (8), 1388–1442. https://doi.org/10.1016/j.pmatsci.2013.03.005.

(42) Huang, F.; Largier, T. D.; Zheng, W.; Cornelius, C. J. Pentablock Copolymer Morphology Dependent Transport and Its Impact upon Film Swelling, Proton Conductivity, Hydrogen Fuel Cell Operation, Vanadium Flow Battery Function, and Electroactive Actuator Performance. *J. Membr. Sci.* **2018**, *545*, 1–10. https://doi.org/10.1016/j.memsci.2017.09.051.

TOC Image Only